0888-8809/02/$15.00/0
Printed in U.S.A.

Molecular Endocrinology 16(6):1243–1256

Expression Profiling in Squamous Carcinoma Cells Reveals Pleiotropic Effects of Vitamin D_3 Analog EB1089 Signaling on Cell Proliferation, Differentiation, and Immune System Regulation

ROBERTO LIN, YOSHIHIKO NAGAI, ROBERT SLADEK, YOLANDE BASTIEN, JOANNE HO, KEVIN PETRECCA, GEORGIA SOTIROPOULOU, ELEFTHERIOS P. DIAMANDIS, THOMAS J. HUDSON, AND JOHN H. WHITE

Departments of Physiology (R.L., Y.N., Y.B., J.H., K.P., J.H.W.), and Medicine (R.S., T.J.H., J.H.W.), McGill University, Montréal, Québec H3G 1Y6, Canada; Montréal Genome Centre (Y.N., R.S., T.J.H.), Montréal General Hospital, McGill University, Montréal, Québec H3G 1A6, Canada; Centre for Nonlinear Dynamics (Y.N.), McGill University, Montréal, Québec H3G 1Y6, Canada; Department of Pharmacology (G.S.), School of Health Science, University of Patras, 26500 Patras, Greece; and Department of Pathology and Laboratory Medicine (E.P.D.), Mount Sinai Hospital and Department of Pathobiology and Laboratory Medicine, University of Toronto, Toronto, Ontario M5G 1X5, Canada

The active form of vitamin D_3, 1α,25-dihydroxyvitamin D_3 [1,25-$(OH)_2D_3$] is key mediator of calcium homeostasis and is a component of the complex homeostatic system of the skin. 1,25-$(OH)_2D_3$ regulates cellular differentiation and proliferation and has broad potential as an anticancer agent. Oligonucleotide microarrays were used to assess profiles of target gene regulation at several points over a 48 h period by the low calcemic 1,25-$(OH)_2D_3$ analog EB1089 in human SCC25 head and neck squamous carcinoma cells. One hundred fifty-two targets were identified, composed of 89 up- and 63 down-regulated genes distributed in multiple profiles of regulation. Results are consistent with EB1089 driving SCC25 cells toward a less malignant phenotype, similar to that of basal keratinocytes. Targets identified control inter- and intracellular signaling, G protein-coupled receptor function, intracellular redox balance, cell adhesion, and extracellular matrix composition, cell cycle progression, steroid metabolism, and more than 20 genes modulating immune system function. The data indicate that EB1089 performs three key functions of a cancer chemoprevention agent; it is antiproliferative, it induces cellular differentiation, and has potential genoprotective effects. While no evidence was found for gene-specific differences in efficacy of 1,25-$(OH)_2D_3$ and EB1089, gene regulation by 1,25-$(OH)_2D_3$ was generally more transient. Treatment of cells with 1,25-$(OH)_2D_3$ and the cytochrome P450 inhibitor ketoconazole produced profiles of regulation essentially identical to those observed with EB1089 alone, indicating that the more sustained regulation by EB1089 was due to its resistance to inactivation by induced 24-hydroxylase activity. This suggests that differences in action of the two compounds arise more from their relative sensitivities to metabolism than from differing effects on VDR function. (*Molecular Endocrinology* 16: 1243–1256, 2002)

NATURALLY OCCURRING VITAMIN D_3 is found in a limited number of dietary sources (*e.g.* cod liver oil, oily fish), and is produced through the action of ultraviolet light on 7-dehydrocholesterol in the skin (1). Vitamin D_3 is one of several factors produced by the complex homeostatic system in the skin, which, as a protective barrier and environmental sensor, is intimately connected to the body's immune and neuroendocrine functions (2). Vitamin D_3 is 25-hydroxylated in the liver and converted into its active 1α,25-dihydroxy form [1,25-$(OH)_2D_3$] in the kidney and several peripheral organs, including skin (2, 3). 1,25-$(OH)_2D_3$ signals through its cognate nuclear vitamin D receptor, which is a direct regulator of gene transcription. Signal transduction by 1,25-$(OH)_2D_3$ has a broad range of physiological effects (2, 3). Primarily, 1,25-$(OH)_2D_3$ controls calcium transport in the intestinal epithelia, and modulates bone resorption. However, it has widespread effects on cellular proliferation and differentiation. 1,25-$(OH)_2D_3$ stimulated differentiation of the OB 17 preadipocyte cell line (4) and induced immature basal layer skin cells to differentiate into keratinocytes (5). Hematopoietic cell lines can be induced to differentiate along the macrophage/monocyte pathway (6–8). 1,25-$(OH)_2D_3$ inhibits proliferation of cells in several models of cancer, including myeloid leukemia, melanoma, and carcinomas of the breast, prostate, colon, and head and neck (3).

Abbreviations: G6PDH, Glucose-6-phosphate dehydrogenase; HNSCC, head and neck squamous cell carcinoma; MMP, metalloproteinase; PTH1R, PTH receptor; SCC, squamous cell carcinoma; SCCA, squamous cell carcinoma antigen; SPC, second primary carcinomas; VDRE, vitamin D response element.

It is unlikely that regulation of a single gene provides the key to the growth inhibitory properties of 1,25-$(OH)_2D_3$ and its analogs. Expression of genes encoding the cyclin-dependent kinase inhibitors $p21^{waf1/cip1}$ and $p27^{kip1}$ was strongly but transiently induced by 1,25-$(OH)_2D_3$ in myeloid leukemia cells, and forced expression of $p21^{waf1/cip1}$ induced myeloid cell differentiation (9, 10). However, the effect of 1,25-$(OH)_2D_3$ on $p21^{waf1/cip1}$ expression varies widely in different cell types. Whereas 1,25-$(OH)_2D_3$ treatment modestly increased $p21^{waf1/cip1}$ protein levels in LNCaP prostate cancer cells, no effect was observed on $p21^{waf1/cip1}$ mRNA or the $p21^{waf1/cip1}$ promoter in these cells (11). Moreover, Hershberger *et al.* (12) and ourselves (13) found that 1,25-$(OH)_2D_3$ repressed $p21^{waf1/cip1}$ expression in mouse head and neck squamous cell carcinoma (HNSCC) lines. The effect of 1,25-$(OH)_2D_3$ on $p27^{kip1}$ expression is generally more consistent. Rapid and transient induction of $p27^{kip1}$ transcripts is accompanied by substantially delayed and more sustained increase in $p27^{kip1}$ protein (10, 14), suggesting that additional mechanisms may control its expression.

The limiting factor for use of 1,25-$(OH)_2D_3$ in cancer therapy has been hypercalcemia. However, many potent analogs have been developed with reduced calcemic effects (15, 16). One such analog, EB1089, contains a side chain modified to render it less susceptible to catabolic degradation (17, 18). *In vivo* studies of prostate and breast carcinomas using EB1089 dosages up to 1.0 μg/kg/d showed no clinically significant hypercalcemia (19, 20). Our previous experiments with a mouse model of HNSCC showed that an EB1089 dose of 0.25 μg/kg/d reduced tumor growth by up to 80% in the absence of hypercalcemia (13).

We are interested in investigating the potential chemopreventive effects of 1,25-$(OH)_2D_3$ analogs using HNSCC as a model. Early stage HNSCC can be successfully treated with surgery and/or radiation therapy. However, primary tumors are often associated with areas of dysplastic epithelia, which lead to the development of second primary carcinomas (SPC) at an annual rate of 3–7%. Thus, it is important to identify chemopreventive agents in HNSCC. Accumulating epidemiological evidence suggests that 1,25-$(OH)_2D_3$ analogs may have widespread chemopreventive effects (16). Preclinical studies with models of colon (16, 22), cheek pouch (23), gastrointestinal (24), and skin carcinogenesis (25, 26) have also provided evidence for chemoprevention. We found that 1,25-$(OH)_2D_3$ and EB1089 induced the expression of the growth arrest and DNA damage (gadd45α) gene in human and mouse HNSCC lines *in vitro* and in tumors by an apparently p53-independent mechanism (13, 21). GADD45α is required for normal DNA repair and maintenance of global genomic stability (27). This strongly suggests that 1,25-$(OH)_2D_3$ and its analogs can act as a genoprotective agents. Induction of DNA repair mechanisms may represent a feedback response to the stimulation of cutaneous vitamin D synthesis by ultraviolet light.

Here, we have used oligonucleotide microarrays to perform large-scale profiling of the effects of EB1089 and 1,25-$(OH)_2D_3$ on gene expression in human HNSCC cells at several times over a 48-h period. Nuclear receptor signaling is ideally suited for microarray analysis, as ligand-bound receptors bind to promoter regions and directly regulate the expression of most of their target genes. These studies provide numerous insights into the effects of 1,25-$(OH)_2D_3$ and its analogs on cell proliferation, differentiation and regulation of immune system function.

RESULTS AND DISCUSSION

Time Courses of EB1089-Regulated Gene Expression in Human SCC25 Cells

We previously found that proliferating human SCC25 HNSCC cells were arrested in G0/G1 by treatment with nanomolar concentrations of EB1089 (21). To determine the molecular events underlying growth arrest, and to assess its potential as a chemopreventive agent, we analyzed the effects of EB1089 treatment on gene expression using Affymetrix HuGene FL oligonucleotide microarrays. SCC25 cells were treated for 0, 1, 2, 6, 12, 24, and 48 h with EB1089 in three independent experiments. Before microarray screening, the response to EB1089 in each experiment was verified by Northern analysis of amphiregulin gene expression (data not shown), as our previous work demonstrated that the amphiregulin gene is a direct target of 1,25-$(OH)_2D_3$ (21, 28).

Compiled raw data was initially analyzed by nonparametric ANOVA (29) to eliminate genes whose change in expression was not statistically significant ($P < 0.05$). Data were then filtered to eliminate genes included because of single chip artifacts, and those with erratic expression profiles that were not consistent between experiments (see below and *Materials and Methods* for details). While previous microarray studies used variation filters as high as 3-fold regulation (30), we chose a filter of 2.5-fold, corresponding to a minimum magnitude change of 200 fluorescence units, so that genes whose induction was similar to that of amphiregulin (average +2.74-fold) would not be excluded. A list of 152 reproducibly regulated EB1089 targets composed of 89 up-regulated and 63 down-regulated genes is presented in Table 1. The results indicate that EB1089 signaling impinges upon every aspect of HNSCC cell function both in terms of intracellular metabolism, and communication with the extracellular milieu.

The list contains a number of previously identified 1,25-$(OH)_2D_3$ targets, including genes encoding integrin α7B, COX-2, and amphiregulin, which were identified in our earlier microarray analysis (21). Sequences encoding another 1,25-$(OH)_2D_3$ target gene in SCC25 cells, $p21^{waf1/cip1}$, are not present on the HuGene FL chip. In addition to 24-hydroxylase, the list also con-

Table 1. List of Genes Regulated by EB1089

		P<0.05	Cluster	Adhesion/cytoskeleton
M69225	+3.2/48	0.00098	U4	*bullous pemphigoid antigen (BPAG1)*
M76482	+2.4/48	0.00009	U5	*desmoglein-3*
M95787	-7.2/48	0.00776	D4	22kDa smooth muscle protein (SM22)
S42303	-6.6/48	0.00132	D4	*N-cadherin*
U47634	+4.3/12	0.00332	U2	beta-tubulin class III
X05608	-4.8/48	0.0002	D2	NF-L
X74929	-5/48	0.00007	D4	keratin 8 (KRT8)
				Cell Cycle
M25753	-2.6/48	0.01613	D4	cyclin B
U66838	-2.9/48	0.0249	D4	cyclin A1
U77949	-2.6/48	0.00056	D3	Cdc6-related protein (HsCDC6)
X51688	-3/48	0.01417	D4	cyclin A
X54942	-2.4/48	0.00035	D3	ckshs2 Cks1 protein homolog
Z36714	-4.2/48	0.0013	D4	cyclin F
				Channels/transporters
L15296	+13.5/12	0.00002	U2	rod cyclic nucleotide-gated cation channel
U73191	-5.3/48	0.00257	D2	inward rectifier potassium channel Kir1.3
U81375	-2.9/24	0.00035	D3	equilibrative nucleoside transporter 1 (hENT1)
				ECM structure/remodeling
HG2197	+2.5/48	0.00749	U4	Collage, Type VII, Alpha 1
M24486	+3.2/48	0.04366	U3	prolyl 4-hydroxylase alpha subunit
M33653	+21.9/48	0.0003	U3	type XIII collagen
M85289	+2.6/48	0.00015	U4	heparan sulfate proteoglycan (HSPG2)
U20758	+6.5/24	0.0002	U3	osteopontin
U50330	+3.5/48	0.00007	U4	procollagen C-proteinase (pCP-2)
U62800	+20/12	0.00045	U2	*cystatin M*
X05232	+9.4/12	0.00749	U3	*stromelysin*
X16832	-4/48	0.00098	D4	cathepsin H
X54925	+14/48	0.00219	U4	*collagenase 1*
X74295	+4.4/48	0.00219	U3	*alpha 7B integrin*
X75308	-20/48	0.00612	D3	*collagenase 3*
X78565	-5/48	0.00797	D3	*tenascin-C, 7560bp*
Z37976	+3.5/48	0.00007	U4	latent TGF binding protein (LTBP-2)
				Immune System
D12763	+26.7/12	0.00533	U3	*T1/ST2*
D38037	+4.2/48	0.00132	U4	FK506-binding protein 12kDa (hFKBP-12) homologue
J04164	-2.6/24	0.01145	D4	interferon-inducible 9-27
M21005	-4.4/48	0.00009	D3	migration inhibitory factor-related protein 8 (MRP8)
M21121	-3.0/24	0	D4	T cell-specific protein (RANTES)
M24594	-1.96/24	0.003	D3	*interferon-inducible 56 Kd*
M26311	-9.2/48	0.00031	D1	migration inhibitory factor-related protein 14 (MRP14)
M29696	-3.3/48	0.00045	D3	IL-7 receptor
M33552	-4.1/48	0.02265	D5	lymphocyte-specific protein 1 (LSP1)
M80254	-2.7/48	0.00219	D2	cyclophilin (hCyP3)
M87507	+2.5/48	0.00009	U3	interleukin-1 beta convertase (IL1BCE)
M93056	+11/48	0.00289	U3	mononcyte/neutrophil elastase inh.
U04343	+4.8/48	0.01613	U5	CD86 antigen
U67615	+2.8/48	0.00582	U3	beige protein homolog chs
U90426	-2.7/48	0.00749	D4	nuclear RNA helicase BAT1
X13334	+27/24	0.0006	U3	CD14 myelid cell-specific glycoprotein
X57351	-2.9/48	0.02539	D5	interferon-inducible 1-8D gene
X59405	+2.8/48	0.00009	U2	Membrane cofactor protein (CD46)
X68487	-2.9/48	0.00009	D2	A2b adenosine receptor
Z49107	+3.5/48	0.00009	U5	galectin
				Intracellular Signaling
D67029	+2.8/48	0.0002	U2	SEC14L
D89016	+2.7/48	0.00219	U4	Rho GEF homolog
HG2167	+2.5/24	0.00058	U3	A-kinase anchoring protein Ht31
L04510	+2.5/48	0.00219	U2	ARD1
L13391	+2.8/48	0.0158	U4	RGS2/G0S8
L15388	+3/48	0.00219	U4	G protein-coupled receptor kinase (GRK5)
M31724	+3.2/48	0.00289	U2	PTP-1B
M58026	+3.5/48	0.00132	U3	NB-1
M61906	+4/48	0	U2	P13-kinase p85
M97815	-4.2/48	0.00045	D2	*CRABP-II*
U02081	+3/48	0.00035	U2	guanine nucleotide regulatory protein NET1
U10550	+6/24	0.00219	U1	Gem GTPase
U15932	+2.5/48	0.00045	U3	dual-specificity protein phosphatase
U40271	+2.7/48	0.01324	U4	receptor tyrosine kinase (PTK7)
U67733	+3.8/24	0.03051	U4	cGMP-stim. 3,5 -cyclic nucleo. Phosphodiesterase PDE2A3(PDE2A)
U96922	+5.2/12	0.00056	U3	inositol polyphosphate 4-phosphatase type II-
X04828	+3.3/48	0.00007	U4	G(i) protein alpha-subunit
X13461	+3.8/48	0.00007	U4	calmodulin-like protein (CLP)
X82676	+3.5/24	0.00439	U2	PEZ/PTP36 tyrosine phosphatase
D00632	+2.8/24	0.00035	U4	**Redox** glutathione peroxidase
D87258	+6/48	0.00098	U4	HtrA chaperon/protease
S73591	+8.2/48	0.00015	U5	VDUP1
V00594	-3.1/48	0.00533	D5	metallothionein from cadmium-treated cells
X55448	+5.8/48	0.00749	U4	*glucose-6-phosphate dehydrogenase (G6PDH)*
X91247	+3/48	0	U1	thioredoxin reductase
Z11793	+4.1/48	0.00009	U4	selenoprotein P
				Signaling peptides/ growth factors
J05008	-5.6/24	0.00318	D1	endothelin-1 (ENT-1)
K03183	-2.6/48	0.01613	D3	chorionic gonadotropin (hcg) beta subunit
M22489	+3.7/48	0.00016	U4	bone morphogenetic protein 2A (BMP-2A)
M30703	+2.7/48	0.00045	U2	*amphiregulin (AR)*
M57293	-2.6/48	0.00749	D3	PTHrP
M60315	+8.1/48	0.00043	U4	transforming growth factor-beta (tgf-beta)
M77140	-4.2/48	0	D4	galanin
M94250	-3.4/48	0.00132	D4	retinoic acid inducible factor (MK)
U03877	-3.1/48	0.01145	D4	*extracellular protein S1-5*
U06863	+2.8/24	0.00045	U4	follistatin-related protein precursor
U43142	-3.2/48	0	D1	*VEGF-related (VRP)*
U62015	-3.6/24	0.00436	D2	Cyr61
X02530	-4/24	0.00098	D3	gamma-interferon inducible IP-10
X57579	-2.6/24	0.01417	D1	activin beta-A subunit
Y00787	-4.1/48	0.00332	D1	monocyte-derived neutrophil chemotactic factor (MDNCF)
				Steroid/lipid metabolism
D28235	+8.2/48	0.00015	U2	Cox-2
J03600	+10.9/48	0.00002	U5	5-lipoxygenase
L11708	+42/48	0.0002	U4	*type 2 17 beta-HSD*
L13286	+196/48	0.0013	U2	*24-hydroxylase*
M91432	+3.2/48	0.00035	U2	medium-chain acyl-CoA dehydrogenase
U05861	+3.1/48	0.00612	U3	*hepatic dihydrodiol dehydrogenase*
U07919	-2.5/48	0.0177	D3	ALDH-6
				Transcription factors
D31716	+2.5/48	0.01016	U5	GC box bindig protein
HG1686	-3/48	0.00098	D5	Transcription Factor E4tf1
HG3510	+2.9/48	0.02265	U4	COUP-TF1
HG4058	-2.6/24	0.01472	D1	Oncogene Aml1-Evi-1
L40387	-2.5/48	0.00332	D3	*TRIP-14*
L49054	+2.7/48	0.00612	U5	fusion gene NPM-MLF1
M19720	+5.2/48	0.00015	U5	L-myc gene
M99701	+3.1/48	0.00007	U3	transc. elongation factor S-II homolog pp21
S74017	+2.6/48	0.00009	U4	*Nrf2 transcriptional activator*
U18018	+2.6/12	0.01324	U3	*E1A enhancer binding protein (E1A-F)*
U63824	-2.7/48	0.00098	D2	transcription factor RTEF-1
U74612	-3.8/48	0.00289	D4	HNF-3/fork head homolog 11
X52611	+4.6/48	0.04366	U4	transcription factor AP-2
X56681	-2.8/24	0.00219	D2	junD
X65644	+3.5/48	0.00805	U2	MHC binding protein 2 (MBP-2)
X82209	+4.4/48	0.00009	U3	MN1 mRNA
X84373	+4.4/24	0.00056	U1	RIP140
				Others
D00408	+36/48	0.00009	U5	*P-450 HFLa*
D17793	+2.6/48	0.01417	U3	KIAA0119
D31883	+3.46/48	0.0002	U3	KIAA0059
D43636	+5.6/12	0.00797	U1	KIAA0096
D76444	+2.8/48	0.00045	U2	hkf-1
D78611	-2.6/48	0.00612	D4	MEST
D86960	+2.9/12	0.00797	U3	KIAA0205
HG4074	-2.6/48	0.00797	D4	XPG
M32053	+4.3/48	0.02539	U5	H19 RNA gene
M60047	-4.5/48	0	D2	*heparin binding protein (HBp17)*
M72885	+4/12	0.0002	U2	G0S2
M90657	-6.2/48	0.00078	D2	tumor antigen (L6)
M93036	-2.5/48	0.01417	D4	carcinoma-associated antigen GA733-2
M97347	-2.7/24	0.00039	D2	Beta-1,6-N-acetylglucosaminyltransferase (AGAT)
S66896	-7.2/48	0.00223	D2	*squamous cell carcinoma antigen (SCCA)*
S81914	-3.5/48	0.00106	D1	*radiation-inducible IEX-1*
S85655	-3.9/48	0.00007	D3	prohibitin
U00115	+3.5/48	0.01324	U5	bcl-6
U08021	-21/24	0.00196	D2	nicotinamide N-methyltransferase (NNMT)
U15174	+3.7/24	0.00078	U4	NIP3
U17077	+2.8/48	0.00039	U3	BENE
U18467	+2.6/48	0.00289	U4	pregnancy-specific beta 1-glycoprotein 7 (PSG7)
U21931	+2.4/24	0.00035	U2	fructose-1,6-biphosphatase
U28369	+31/48	0.00035	U3	*semaphorin 3B (sema3B)*
U38276	+2.9/48	0.00132	U3	semaphorin 3F (Sema 3F)
U51010	-9.5/24	0.01106	D2	nicotinamide N-methyltransferase
U52100	-3/24	0.00132	D3	XMP
U52101	-3.6/48	0.00007	D3	*YMP*
U62801	+32/24	0.00257	U3	*protease M*
U95740	+5.7/48	0.00612	U3	362G6.2 from BAC clone chromosome 16p13.1
X06561	+2.8/48	0.00612	U5	27-kDa calbindin
X12517	-4.3/48	0.00561	D4	U1 small nuclear RNP-specific C protein
X14850	-2.6/48	0.00098	D4	histone H2A.X
Y00339	+5.1/48	0.00257	U3	carbonic anhydrase II
Y00757	-2.9/24	0.01661	D4	polypeptide 7B2
Z25535	-2.6/48	0.00257	D3	*nuclear pore complex protein hnup153*
Z29331	+2.7/48	0.00228	U5	(23k/3) ubiquitin-conjugating enzyme UbcH2

The GenBank accession no. for each gene is provided in the *first column*. The *second column* lists the maximum fold regulation and time of maximal activation. The *third column* gives *P* value derived from nonparametric ANOVA. Note that *P* values of less than 0.00001 are listed as 0. The *fourth column* gives the cluster number derived in Fig. 2. Genes whose regulation has been confirmed by RT-PCR analysis and/or Northern blotting are in *italics*. The profiles of individual experiments used to compile the above data are shown in Table 2, which is published as supplemental data on The Endocrine Society's Journals Online web site, http://mend.endojournals.org/.

tains other vitamin D-responsive genes including those encoding osteopontin, carbonic anhydrase II, VDUP1 (vitamin D up-regulated 1), PTHrP, CD14, and TGFβ (31–38). One exception is the gene encoding GADD45α, which we showed is 1,25-$(OH)_2D_3$ responsive in mouse and human HNSCC lines (13, 21). Although it appeared up-regulated, the gadd45α gene was not retained during the filtering process because

of elevated levels of nonspecific hybridization to control oligonucleotide sets (data not shown).

The range of fold regulation of target genes varied widely, with 24-hydroxylase exhibiting by far the highest up-regulation (196-fold at 48 h) of all genes identified. Expression of eight of these genes representing a range of fold regulations was further analyzed by Northern blotting (Fig. 1). The results of Northern and microarray analyses are in very good agreement. Most importantly, regulation of all genes identified on microarrays was confirmed on Northern blots, and the relative magnitudes of fold regulation observed were the same using the two techniques. There was also broad agreement between the fold regulations observed using the two techniques. The exceptions were cystatin M and protease M, where fold inductions at 24 h of 6.7- and 18-fold, and 8- and 32-fold were observed by Northern blotting and microarray analysis, respectively. However, other differences in fold regulation were less than 2-fold. Taken together, these experiments, coupled with RT-PCR analysis (Table 1, and see below), suggest that while the absolute magnitudes of fold regulation detected by microarray analysis may be somewhat higher in some cases than

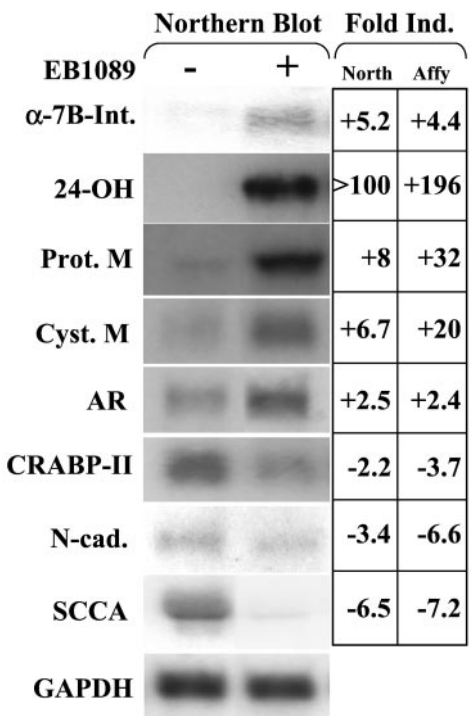

Fig. 1. Northern Analysis of EB1089 Target Gene Regulation

Northern analyses were performed on RNA extracted from control SCC25 cells or cells treated for 24 h with EB1089. Blots were hybridized with probes specific for integrin α-7B (α-7B), 24-hydroxylase (24-OH), protease M (prot. M), cystatin M (cyst. M), amphiregulin (AR), CRABP-II, N-cadherin (N-cad.), squamous cell carcinoma antigen (SCCA), and GAPDH control. Comparison of fold regulations after 24 h detected by Northern blotting (North) and Affymetrix microarrays (Affy) are provided.

those detected by other techniques, the data compiled in Table 1 is highly reliable.

Initial clustering analysis of averaged data of reproducibly regulated genes processed by the K-mean algorithm with k=5 generated 4 clusters of up-regulated genes distinguished based on rapidity of induction (data not shown). No such resolution was achieved for down-regulated genes, arising from fact that the absolute value of the average fold activation of the up-regulated genes at any given time point was substantially greater than that of the down-regulated genes. In addition, the K-mean algorithm is strongly dependent upon the choice of initial points (K number of initial conditions). Therefore, different initial points will have different nearest neighbors, and refinement of calculating means with various neighbors can generate different clusters starting from different initial conditions.

We have developed a method of clustering analysis that does not take into account initial conditions, and categorizes genes based on time of crossing of a threshold value (see *Materials and Methods* for details). The method generated symmetrical groups of clusters of up- and down-regulated genes (Fig. 2, A–L). The profiles of cluster genes were generally much less erratic than genes eliminated by filtering (Fig. 2, M and N). For example, the compiled data for E2F4 (a transcription factor controlling cell cycle progression), which suggests rapid up-regulation, is composed of three distinctly different profiles (Fig. 2O). Indeed, analysis of E2F4 transcripts from EB1089 treated cells by RT-PCR revealed no regulation (Fig. 2O, *inset*).

The 24-hydroxylase gene is among the most rapidly regulated genes in cluster U1, whereas regulation of the osteopontin gene is significantly slower (cluster U3; Fig. 2, Table 1). The promoters of both of these genes contain vitamin D response elements (VDREs) (31, 32). In addition, regulation of the carbonic anhydrase II gene, whose chicken homolog contains a VDRE (33), fell into cluster U3. This indicates that the kinetics of gene induction by the EB1089/VDR bound to different VDREs is strongly promoter specific. Several cell cycle regulatory genes whose products function after the G1/S boundary were among the more slowly regulated genes in clusters D3 and D4 (Table 1), likely reflecting the gradual diminution of cells in S phase or later. This is supported by observations that cyclin A1 and cyclin B levels in cells in G2 do not change during EB1089 treatment (not shown).

Regulation by EB1089 of Markers Associated with Cancer Cell Progression

EB1089 signaling regulates the expression of several markers associated with progression of cancer phenotypes. Of genes whose expression is reduced or eliminated in cancer cells, almost all are up-regulated by EB1089 (Fig. 3A). Two of the more strongly induced genes, kallikrein protease protease M and the cysteine protease inhibitor cystatin M (Table 1 and Fig. 3A), are down-regulated in breast cancers (39, 40), as is calm-

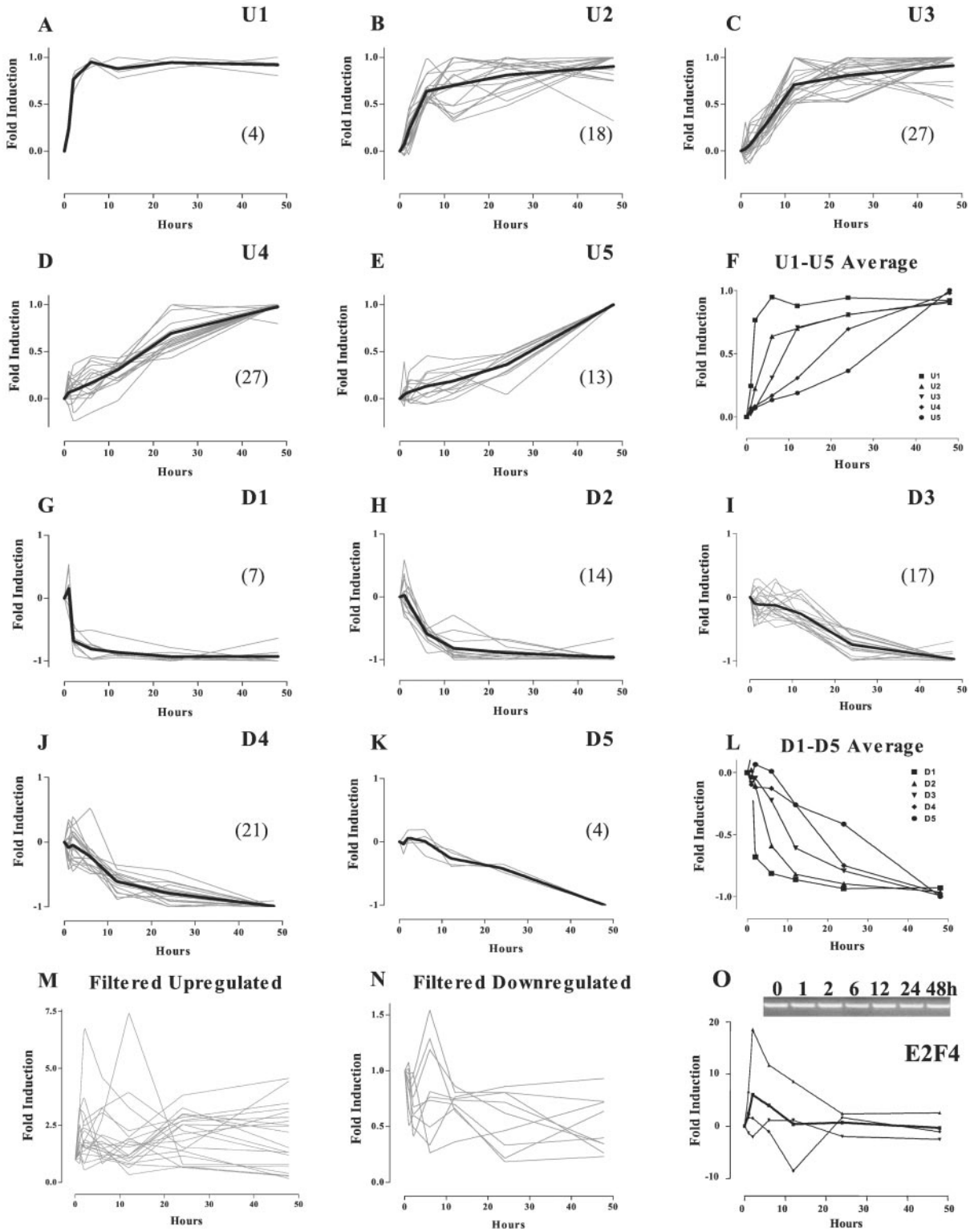

Fig. 2. Profiles of Genes Listed in Table 1 were Subjected to Clustering Analysis

A–E, Normalized profiles of up-regulated genes in clusters U1–U5 are presented, with the average trace shown in *bold*. F, Comparison of the average profiles for clusters U1–U5. G–K. Normalized profiles of down-regulated genes in clusters D1–D5 are presented, with the average trace shown in *bold*. L, Comparison of the average profiles for clusters D1–D5. Numbers of genes in each cluster are indicated in *brackets*. M, N, Profiles of up- and down-regulated genes eliminated by filtering before clustering analysis (see *Materials and Methods* for details). O, Analysis of transcription factor E2F4 regulation in EB1089-treated cells. The composite profile (in *bold*) and individual data sets are shown. The *inset* shows an analysis of E2F4 transcripts from EB1089-treated cells by RT-PCR using the same RNA preparations as in Fig. 5.

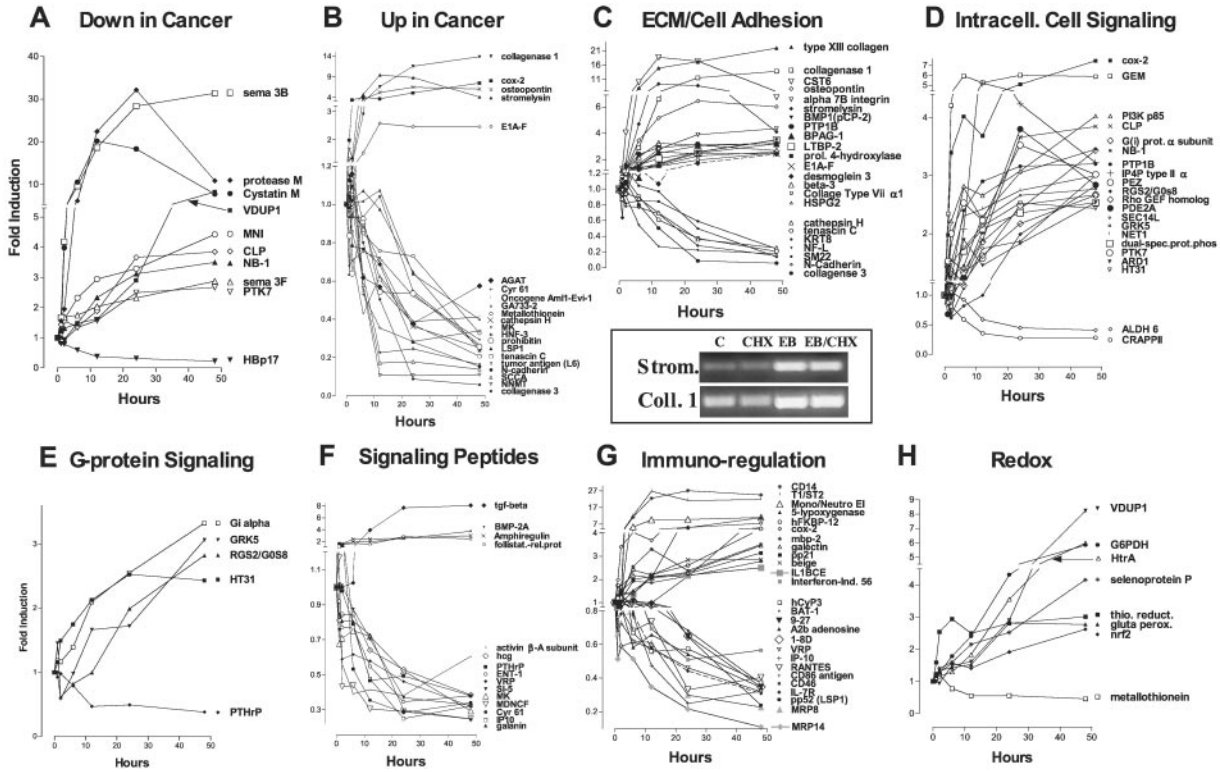

Fig. 3. Profiling of EB1089-Regulated Gene Expression

A, EB1089-dependent regulation of genes whose expression is generally disrupted or down-regulated in cancer. B, Genes whose expression is up-regulated in cancer. C, Genes controlling extracellular matrix structure and cell adhesion. *Bottom*, Cycloheximide does not block EB1089-dependent induction of collagenase 1 and stromelysin gene expression. SCC25 cells were treated with cycloheximide (C), and EB1089 (E) alone or in combination as indicated for 24 h. Total RNA was analyzed by RT-PCR for expression of stromelysin, collagenase 1. GAPDH expression was not affected (not shown). D, Genes controlling non-GPCR-mediated intracellular signaling. E, Genes modulating GPCR function. F, Genes encoding signaling peptides. G, Genes controlling regulation of immune system function. H, Genes controlling intracellular redox balance. Note that these categories are not mutually exclusive, and some genes may appear under more than one category. In addition, not all genes listed in Table 1 are presented.

odulin-like protein (41). Calmodulin-like protein is a marker of epithelial cell differentiation (41). Genes encoding semaphorin 3B and 3F lie in a region of chromosome 3 deleted in lung cancers (42–44). The exception to the above is HBp17, a putative regulator of FGF signaling that was expressed at lower levels in SCC than in primary cultures of keratinocytes (45).

EB1089 also down-regulates a large number of genes that are overexpressed in cancers (Fig. 3B), including tumor antigen L6, carcinoma associated antigen GA733-2, and squamous cell carcinoma antigen (SCCA). SCCA is a serum marker of uterine cervix, head and neck, lung, and esophageal cancers, and ablation of its expression inhibits growth and induces natural killer cell infiltration of tumors (46). Another down-regulated gene, tenascin C, is an early marker of HNSCC progression (47) Similarly, repression of overexpressed N-cadherin in head and neck squamous cell carcinoma is associated with restoration of an epithelial phenotype (48).

The above results suggest that EB1089 treatment reversed the malignant phenotype of SCC25 cells. This possibility was investigated further by immunofluorescence analysis of three markers that are differentially expressed in cancer cells, cystatin M, protease M, and N-cadherin. Both protease M and cystatin M transcripts are strongly induced by EB1089, and cystatin M is an ideal marker for these purposes because its expression is highly specific for differentiated epidermal keratinocytes (49). In addition, up-regulation of N-cadherin in head and neck squamous, breast and prostate cancers ("cadherin switching") is associated with cancer progression, invasion and metastasis (48, 50, 51). Immunofluorescence studies in control and EB1089-treated cells (Fig. 4) revealed a strong up-regulation of cystatin M expression, giving rise to strong, relatively uniform cytoplasmic staining (Fig. 4, A and B). Similar results were obtained with immunofluorescence analysis of protease M expression (Fig. 4, C and D), with the exception that elevated levels of protease M expression varied somewhat in EB1089-treated cells. In contrast, EB1089 treatment down-regulated N-cadherin expression (Fig. 4, E and F). This down-regulation included cell-cell contact sites, as well as the dotted pattern of non-cell-to-cell contacts seen in other carcinoma cells (51). The changes observed are in excellent agreement with the regulation of the genes encoding these markers (Table 1, Figs. 1 and 3). Moreover, in addition to providing evidence

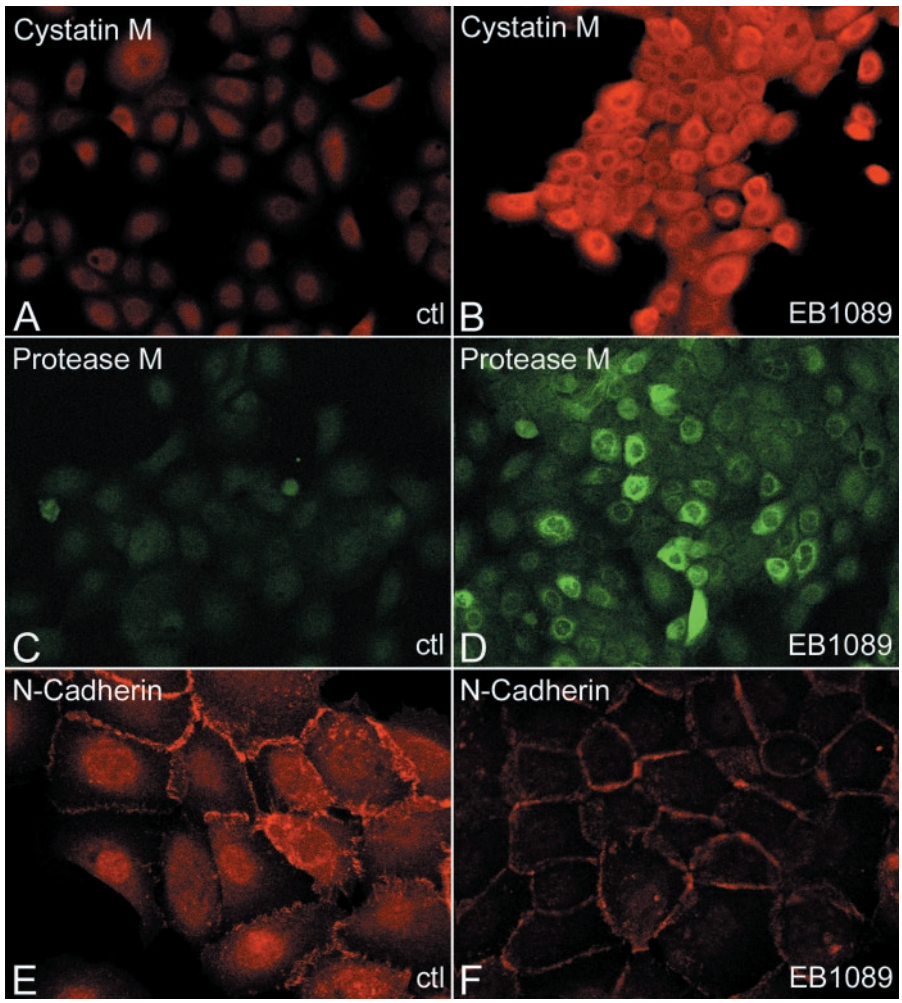

Fig. 4. Immunofluorescence Analysis of Cystatin M, Protease M, and N-Cadherin Expression in EB1089-Treated SCC25 Cells

Control (ctl; vehicle-treated) and EB1089-treated SCC25 cells were analyzed by immunofluorescence for expression of cystatin M (A and B), protease M (C and D), and N-cadherin (E and F). Primary antibodies were detected with Cy3-conjugated goat antirabbit (A, B, E, and F) or Cy2-conjugated goat antimouse (C and D) secondary antibodies. No staining was seen in the absence of primary antibodies (data not shown). Images of each control and EB1089-treated sample pair were acquired by confocal microscopy and processed using identical parameters. See *Materials and Methods* for details. Magnifications: A–D, ×25; E and F, ×63.

that EB1089 reverses the malignant phenotype of SCC25 cells, these studies provide sensitive new markers for HNSCC progression and treatment.

Regulation of Genes Controlling ECM Structure and Remodeling, and Cell Adhesion Consistent with Induction of a Basal Keratinocyte Phenotype

EB1089 does induce expression of some genes that are often up-regulated in cancers, many of which are implicated in extracellular matrix (ECM) structure and remodeling. Up-regulated genes include those encoding transcription factor E1A-F, which controls matrix metalloproteinase (MMP) gene expression (52), and two of its target genes, MMPs stromelysin and collagenase 1 (Fig. 2, B and C). EB1089-dependent induction of stromelysin, collagenase 1 and E1A-F was confirmed by RT-PCR (Figs. 2 and 3). Although E1A-F is a regulator of collagenase gene expression, cycloheximide did not block EB1089-induced expression of collagenase 1 or stromelysin (Fig. 3C, *bottom*). This indicates that induction of E1A-F expression by EB1089 is not essential for observed regulation of collagenase 1 and stromelysin, and that EB1089 has both long- and short-term effects on matrix metalloproteinase expression. Expression of osteopontin, a noncollagen matrix protein implicated in ECM structure and remodeling was also up-regulated. Several studies have indicated that osteopontin, collagenase 1, and stromelysin play key roles in ECM remodeling during wound healing (53–55). Up-regulation of their expression by EB1089 provides a molecular genetic basis for the proposed stimulatory role of 1,25-$(OH)_2D_3$ in wound healing (56).

The strong induction (22-fold) of expression of the type XIII collagen gene, a transmembrane collagen, provided further evidence that EB1089 induced kera-

tinocytic differentiation of SCC25 cells. Interestingly, trimerization of type XIII collagen is activated by prolyl 4-hydroxylase (57), whose gene is also up-regulated (Fig. 3C). Type XIII collagen is expressed in normal human epidermis and is present at cell-to-cell contact sites and at the dermal-epidermal junction. It is highly colocalized with E-cadherin and may be a component of adherens-like junctions (58). In addition, expression of phosphotyrosine phosphatase PTP-1B, whose activity has been associated with enhanced cell adhesion (59), is also increased.

EB1089 also up-regulates BPAG-1 (bullous pemphigoid antigen-1; Fig. 3C), a component of hemidesmosomes, structures essential for adhesion of epithelial cells to basement membranes (60). Absence or disruption of hemidesmosomal components gives rise to devastating bullous pemphigoid blistering skin disorders. EB1089 also induces expression of desmoglein 3 (Fig. 3C), a cadherin component of desmosomes (60), and the autoantigen in pemphigus vulgaris. It is noteworthy that desmogleins are expressed in a gradient in the epidermis, with desmoglein 3 most abundant in the basal layer (61). This observation, coupled with the up-regulation of type XIII collagen and hemidesmosomal components, provides further evidence that EB1089 induces a more epithelial, less malignant phenotype in SCC25 cells, consistent with that of basal keratinocytes.

Pleiotropic Effects of EB1089 on Inter- and Intracellular Signaling

Expression of several factors controlling intracellular signaling was altered in EB1089-treated cells (Figs. 2, D–F), including a number of genes encoding proteins controlling G protein-coupled receptor signaling (Fig. 3E). Up-regulated genes include those encoding the A kinase anchoring protein Ht31, and RGS2/G0S8, which is a selective inhibitor of Gq α signaling (62). The induction of RGS2/G0S8 is intriguing, as its expression is also induced by PTH in bone (63), which can signal through a G protein-coupled receptor linked to Gq α (64). 1,25-$(OH)_2D_3$ represses PTH receptor (PTH1R) signaling by inhibiting expression of the receptor and ligands PTH and PTHrP (Fig. 3F; Refs. 34, 35, 65). In addition, EB1089 treatment induces expression of the G receptor kinase GRK5 (Fig. 3E), which can repress PTH1R function (66). These results indicate that, in addition to inhibiting ligand and receptor expression, 1,25-$(OH)_2D_3$ signaling can also repress PTH1R function by inducing expression of factors that inhibit signaling via Gq α.

Expression of a number of signaling peptides was altered in treated cells (Fig. 3F), emphasizing the neuroendocrine nature of epidermal function (2). Our previous studies have shown that induction of amphiregulin (Fig. 3G) can inhibit SCC25 proliferation (28). Down-regulated genes include galanin, a neuropeptide implicated in nerve regeneration after injury (67), and S1–5, a relatively uncharacterized factor with EGF-like domains (68). Consistent with its antiproliferative effects, EB1089 down-regulated expression of several mitogenic factors. These include VEGF-related protein, which is mitogenic in Kaposi's Sarcoma and hematopoietic cells (69, 70), Cyr61, which encodes a growth factor implicated in angiogenesis and tumorigenesis, whose expression is induced by estrogen in breast cancer cells (71), and midkine, mitogenic factor overexpressed in several carcinomas (72).

Regulation of Genes Controlling Immune System Function

Keratinocytes are considered to be an integral part of the immune system of the skin (2). The intimate connection of epithelial cells to immune system function is reinforced by the large number of EB1089-related genes in SCC25 cells implicated in immunoregulation (Fig. 3G). The role of 1,25-$(OH)_2D_3$ in controlling the function of epithelial cells in innate immunity (73) is underlined by the strong induction by EB1089 of the gene encoding the pattern receptor CD14 (Fig. 3H), which is also a target gene in monocytic HL60 cells (37). Significantly, another strongly induced gene is that encoding T1/ST2, a member of the IL-1 receptor family. Gene ablation studies in mice have revealed that T1/ST2 signaling is required for T helper 2, Th2, cell differentiation (74).

EB1089 down-regulated interferon γ-regulated genes encoding 9–27, 1–8D, interferon-inducible 56K protein, and the T cell chemokine IP-10, and the chemokine RANTES, which is also overexpressed in a number of cancers including more advanced breast cancer (75). Interferon γ signaling and overexpression of IP-10 underlie the inflammatory reactions in psoriasis (76). Previous studies have suggested that 1,25-$(OH)_2D_3$ signaling can influence T helper cell differentiation (3). These data indicate that directs effects on epithelial cell signaling play a key role in the antiinflammatory action of 1,25-$(OH)_2D_3$ analogs in skin. Our results are consistent with EB1089 stimulating Th2 responses, and inhibiting a number of genes associated with proinflammatory Th1 responses.

Control of Genes Regulating Cellular Redox Balance

EB1089 signaling regulates a number of genes encoding proteins that control cellular redox balance (Fig. 3H). Induction of these genes by EB1089 and 1,25-$(OH)_2D_3$ may represent a feedback response to epidermal vitamin D_3 synthesis induced by sunlight, which is an effective inducer of reactive oxygen species in skin (77, 78). Up-regulated genes include glucose-6-phosphate dehydrogenase (G6PDH), selenoprotein P, glutathione peroxidase, thioredoxin reductase, HtrA, and, importantly, the nrf2 transcription factor. Selenoprotein P is a plasma heparin binding protein with antioxidant properties (79). HtrA is an extremely well conserved protein whose prokaryotic homolog is essential for survival under conditions of

oxidative stress (80). Ablation of nrf2 expression in mice rendered them more susceptible to carcinogenesis and resistant to the protective effects of chemoprevention agents (81). Nrf2 expression, which is induced by a number of chemopreventive agents, in turn induces expression of a number of phase II detoxifying enzymes. These events may provide a mechanism for protection by 1,25-$(OH)_2D_3$ against dimethyl-benzanthracene carcinogenesis in hampster cheek pouch carcinoma (24). Dimethyl-benzanthracene is activated by a series of oxidation steps, and detoxified by phase II enzymes (82).

Both G6PDH and thioredoxin reductase contribute to nucleotide biosynthesis in proliferating cells and are overexpressed in cancer cells (83, 84). However, in quiescent cells they are source of reducing equivalents. G6PDH is at the head of the pentose-phosphate shunt, which is a source of NADPH, and thioredoxin reductase uses NADPH to reduce thioredoxins, proteins that in turn reduce oxidized cysteines. Elevated G6PDH and thioredoxin levels protect against apoptosis, which is sensitive to redox balance. Recent studies have shown that short-term 1,25-$(OH)_2D_3$ treatment of MCF-7 breast cancer cells has prooxidant effects (85). However, unlike the results of obtained in SCC25 cells (Fig. 3), G6PDH induction in MCF-7 cells was modest, and no changes in glutathione peroxidase levels were found. Significantly, however, 1,25-$(OH)_2D_3$ is an effective inducer of apoptosis in MCF-7 cells, whose onset can be controlled by redox balance, whereas no evidence for apoptosis was found in 1,25-$(OH)_2D_3$-treated SCC25 cells (21). This suggests that the effects of 1,25-$(OH)_2D_3$ on redox balance may be cell specific.

EB1089 and 1α,25$(OH)_2D_3$ Regulate Target Gene Expression with Similar Efficacy

We have confirmed the regulation of a total of 30 genes by Northern blotting and/or RT-PCR (Figs. 1 and 5, Table 1). In addition to the 17 genes presented in Fig. 5, regulation of 9 other genes was confirmed at single time points (Table 1, and data not shown). We have also compared regulation by EB1089 and 1,25-$(OH)_2D_3$ of several target genes. Structure/function studies have suggested the VDR forms structurally distinct complexes with EB1089 and 1,25-$(OH)_2D_3$, possibly providing a molecular basis for gene-specific effects of the two compounds (86). In preliminary analyses by RT-PCR of the effects of 24 or 48 h treatment with EB1089 or 1,25-$(OH)_2D_3$, several target genes analyzed appeared to be differentially regulated by two compounds (data not shown). Therefore, we compared target gene regulation by EB1089 and 1,25-$(OH)_2D_3$ over the entire 48 h time course (Fig. 5). The results showed that 1,25-$(OH)_2D_3$ regulated expression of several genes more transiently than EB1089 but did not provide any evidence for gene-specific differences in efficacy of the two compounds (Fig. 5).

To examine the potential role of 24-OHase in attenuation of 1,25-$(OH)_2D_3$ signaling by 48 h, we compared expression profiles in SCC25 cells treated with vehicle, EB1089 or 1,25-$(OH)_2D_3$ in the presence or absence of the cytochrome P450 inhibitor ketoconazole (Fig. 6). As expected, induction of T1/ST2 expression by EB1089 after 48 h was strong, and was unaffected by ketoconazole. In contrast, while the effect of 1,25-$(OH)_2D_3$ alone after 48 h was weaker, T1/ST2 expression remained high in cells treated with 1,25-$(OH)_2D_3$ and ketoconazole together and was essentially identical to that observed in the presence of EB1089 or EB1089 and ketoconazole. Similar effects of ketoconazole were observed on 1,25-$(OH)_2D_3$-dependent induction of semaphorin 3B, and type II 17β-hydroxysteroid dehydrogenase genes, and on repression of the SCCA gene (Fig. 6). No effects were observed of ketoconazole alone or with ligands on GAPDH expression (not shown). Thus, the more sustained regulation of several target genes by EB1089 is likely due to its insensitivity to induction of 24-OHase activity. The variability observed in the relative durations of the regulatory effects of EB1089 and 1,25-$(OH)_2D_3$ in Fig. 5 may reflect differences in stability of association of ligand-bound VDR with specific promoters, or with differing stabilities of target gene mRNAs. The data do not provide any evidence for gene-specific differences in efficacy of *trans*-activation or -repression by EB1089 and 1,25-$(OH)_2D_3$.

CONCLUSIONS

The studies above provide multiple insights into not only the potential of 1,25-$(OH)_2D_3$ analogs as agents of cancer chemoprevention, but also into the physiological actions of 1,25-$(OH)_2D_3$ in a number of tissues, including skin, bone, and the immune system. The data indicate that EB1089 performs key functions of a cancer chemoprevention agent; it is antiproliferative, it induces cellular differentiation, and it has potential genoprotective effects over and above our previous findings of the induction of GADD45α (13, 21). Differential effects on gene expression of EB1089 and 1,25-$(OH)_2D_3$ were attributable to the insensitivity of EB1089 to 24-OHase activity, suggesting that differences in action of the two compounds arise more from their sensitivity to metabolism and than from differential action of the VDR bound to each ligand.

MATERIALS AND METHODS

Tissue Culture and RNA Extraction

SCC25 cells were obtained from the American Type Culture Collection (Manassas, VA), and were cultured under recommended conditions. Cells cultured in 10-cm plates under conditions where controls cell could proliferate for at least 10 d before confluence (21). Media were changed 24 h before treatment with EB1089 or 1,25-$(OH)_2D_3$ (100 nM) in dimethylsulfoxide for 0, 1, 3, 6, 12, 24, or 48 h as previously de-

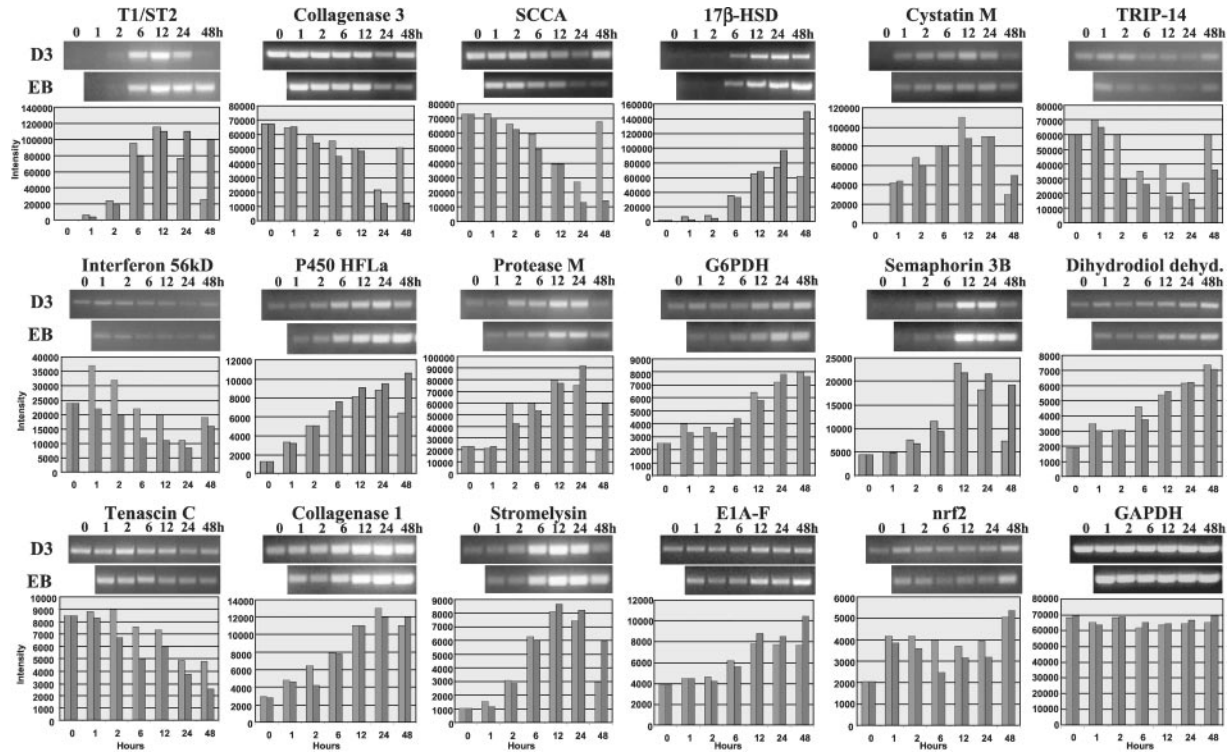

Fig. 5. Comparison of Effects of EB1089 and 1,25-$(OH)_2D_3$ on Target Gene Expression

SCC25 cells were cultured and treated with in parallel with EB1089 (*dark gray bars*) or 1,25-$(OH)_2D_3$ (*pale gray bars*) as indicated and gene expression was analyzed by RT-PCR. Genes selected included both up- and down-regulated targets and strongly (*e.g.* T1/ST2, protease M) and moderately (*e.g.* E1A-F, interferon-inducible 56-kDa protein) regulated genes.

scribed (21). Total RNA was extracted with TRIZOL (Life Technologies, Inc., Burlington, Ontario, Canada), and 10 μg of RNA isolated from EB1089-treated cells were used for microarray analysis. Cycloheximide (200 nM; Sigma-Aldrich Canada, Oakville, Ontario, Canada) was added 1 h before addition of EB1089 as indicated. Ketoconazole (100 nM; Sigma-Aldrich Canada) was added along with EB1089 and 1,25-$(OH)_2D_3$ as indicated.

Microarray Screening and Data Analysis

Probe for microarray analysis was generated, and Affymetrix HuGene FL human gene oligonucleotide microarrays were screened as described in Novak *et al.* (87). Screenings for EB1089-regulated genes were performed with three sets of probes generated from three independent tissue culture experiments. To test for statistically significant changes in signal intensity, compiled data was screened initially by nonparametric ANOVA (29) using a P value of < 0.05. Genes retained were then filtered for those whose expression was up- or down-regulated a minimum of 2.5-fold at some point during the 48-h time course, corresponding to a minimum magnitude change of 200 fluorescence units. The data were filtered to eliminate genes with noisy expression profiles by calculation of cross correlations between individual profiles and hyperbolic tangents [$x(t)=tanh(nt/2)$], where x is normalized fold induction, t is time, and n is a time constant controlling time of saturation. Profiles of up-regulated genes with correlation coefficients of 0.8 or less, and down-regulated genes with correlation coefficients of less than -0.8 were eliminated.

A method of clustering analysis was developed that classifies groups of genes based on time of regulation with respect to a threshold value, and does not take into account initial conditions. Maximal gene regulation was normalized to 1 for up-regulated genes and -1 for down-regulated genes. Given that experimental measurements were performed at 0, 1, 2, 6, 12, 24, and 48 h, the number of intervals initially generates 6 clusters each for up- and down-regulated genes. Clustering was evaluated for threshold values between 0.25 and 0.75, and -0.25 and -0.75 for induced and repressed genes, respectively. The number of clusters was then heuristically adjusted based on the following criteria: 1) a cluster must contain at least two genes; 2) the mean value of each cluster does not cross that of another cluster near the threshold. The optimum threshold was chosen as that generating the maximum cluster stability defined by the probability of a gene belonging to the same cluster in the average data set and the individual data sets. Based on these criteria, 0.50 and -0.50 were chosen as threshold values. The time the threshold is crossed was computed using a linear interpolation method. To avoid multiple threshold crossings, only the first crossing with a positive derivative for up-regulated genes, and negative derivative for down-regulated genes were considered. Analysis was carried out using Mathlab 6.12 (MathWorks Inc., Natick, MA).

Immunofluorescence

SCC25 cells were plated on cover slips and treated with dimethylsulfoxide vehicle or 100 nM EB1089 for 72 h. Cells were processed for immunolabeling as described in (88). Briefly, cells were fixed in 2% paraformaldehyde and permeabilized, and blocked with Triton X-100/BSA. Cells were sequentially labeled with affinity purified rabbit anticystatin M (1:50; Refs. 40, 49), mouse antiprotease M (1:150; Ref. 89) or rabbit anti-N-Cadherin (1:50; Sigma) primary antibodies for 1 h at room temperature followed by Cy3-conjugated goat antirabbit or Cy2-conjugated goat antimouse secondary antibodies (Jackson ImmunoResearch Laboratories, Inc., West

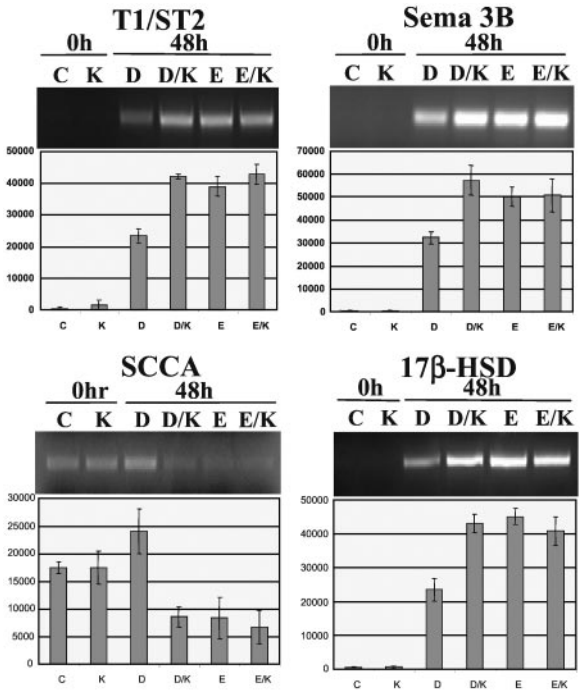

Fig. 6. Analysis of the Effects of Cytochrome P450 Inhibitor Ketoconazole on EB1089- and 1,25-$(OH)_2D_3$-Regulated Gene Expression

SCC25 cells were treated with vehicle alone (control; C), 100 nM ketoconazole alone (K), 100 nM 1,25-$(OH)_2D_3$ alone (D), 100 nM EB1089 alone (E), or in combination as indicated. Total RNA isolated from treated cells was analyzed by RT-PCR for expression of T1/ST2, Semaphorin 3B (Sema 3B), 17β-hydroxysteroid dehydrogenase (17β-HSD), and SCCA. Results of three independent experiments are presented.

Grove, PA) for 1 h at room temperature. Immunofluorescence was visualized with a Bio-Rad Laboratories, Inc. (Hercules, CA) MicroRadiance confocal microscope at an optical thickness of approximately 10 μm using 25− or 63− objectives. For each pair of control and EB1089-treated samples, images were acquired and processed using identical parameters. Digital images were prepared using Adobe Photoshop.

Northern Blotting and RT-PCR Analysis of Regulated Gene Expression

Total RNA was extracted from SCC25 cells using Trizol (Life Technologies, Inc.). Denatured RNA (3 μg) was reverse transcribed in a 20 μl reaction at 42 C for 50 min with SuperScript II (Life Technologies, Inc.) according to the supplier's instructions. Amplification conditions were optimized in preliminary experiments so that maximal amplification fell within the linear range. Products were diluted to 200 μl, denatured at 95 C for 2 min, and then amplified as follows: Tenascin C, (27 cycles; 94 C, 30 sec; 57.5 C, 45 sec; 72 C, 45 sec) with forward 5′-CCACAGCTGGGAGATTTAGC-3′ and reverse 5′-CTGGGAGCAAGTCCAGAGAG-3′ primers; Nrf2, (21 cycles; 94 C, 30 sec; 57.5 C, 45 sec; 72 C, 45 sec) with forward 5′-ACCCTTGTCACCATCTCAGG-3′ and reverse 5′-TTGCCATCTCTTGTTTGCTG-3′ primers; dihydrodiol dehydrogenase, (21 cycles; 94 C, 30 sec; 57.5 C, 45 sec; 72 C, 45 sec) with forward 5′-GGTCACTTCATGCCTGTCCT-3′ and reverse 5′-GGATGACATTCCACCTGGTT-3′ primers; stromelysin (27 cycles; 94 C, 30 sec; 57.5 C, 45 sec; 72 C, 45 sec) with forward 5′-AACCTGTCCCTCCAGAACCT-3′ and reverse 5′-TGGGTCAAACTCCAACTGTG-3′primers; Collagenase 1, (27 cycles; 94 C, 30 sec; 57.5 C, 45 sec; 72 C, 45 sec) with forward 5′-TGGACCTGGAGGAAATCTTG-3′ and reverse 5′-GGGGTATCCGTGTAGCACAT-3′ primers; E1AF, (27 cycles; 94 C, 30 sec; 57.5 C, 45 sec; 72 C, 45 sec) with forward 5′-CGCCTACGACTCAGATGTCA-3′ and reverse 5′-GGAAGGCCAAAGAGAAGAGG-3′primers; Protease M, (27 cycles; 94 C, 30 sec; 57.5 C, 45 sec; 72 C, 45 sec) with forward 5′-GGGGTCCTTATCCATCCACT-3′ and reverse 5′-GGGATGTTACCCCATGACAC-3′ primers; G6PD, (27 cycles; 94 C, 30 sec; 57.5 C, 45 sec; 72 C, 45 sec) with forward 5′-CAACCACATCTCCTCCCTGT-3′ and reverse 5′-TCCCACCTCTCATTCTCCAC-3′ primers; ST2, (27 cycles; 94 C, 30 sec; 57.5 C, 45 sec; 72 C, 45 sec) with forward 5′-CAACTGGACAGCACCTCTTG-3′and reverse 5′-CAAATTCAGGGCCAGACAGT-3′ primers; P-450 (27 cycles; 94 C, 30 sec; 57.5 C, 45 sec; 72 C, 45 sec) with forward 5′-TTGCCCAGTATGGAGATGTG-3′ and reverse 5′-GAACACTGCTCGTGGTTTCA-3′ primers; 17β-hydroxysteroid dehydrogenase, (27 cycles; 94 C, 30 sec; 57.5 C, 45 sec; 72 C, 45 sec) with forward 5′-CACGAAGCCAGTGCAGATAA-3′ and reverse 5′-GGAAATTCCGCTGTGCTAAG-3′ primers; Cystatin M (27 cycles; 94 C, 30 sec; 57.5 C, 45 sec; 72 C, 45 sec) with forward 5′-GGAGAACTCCGGGACCTGT-3′ and reverse 5′-GGAACCACAAGGACCTCAAA-3′ primers; Semaphorin V, (33 cycles; 94 C, 30 sec; 60 C, 45 sec; 72 C, 45 sec) with forward 5′-AACCTGTGCCTTTGTGGAAG-3′ and reverse 5′-AGCTGATCGAAGTGGGTGTC-3′ primers; Collagenase 3 (26 cycles; 94 C, 30 sec; 57.5 C, 45 sec; 72 C, 45 sec) with forward 5′-ATGACTGAGAGGCTCCGAGA-3′ and reverse 5′-ACCTAAGGAGTGGCCGAACT-3′ primers; TRIP-14, (26 cycles; 94 C, 30 sec; 57.5 C, 45 sec; 72 C, 45 sec) with forward 5′-AAAGAGAGGCCATCATCCT-3′ and reverse 5′-CAGGAACCTGGAAGGACAGA-3′ primers; VEGF-related protein (33 cycles; 94 C, 30 sec; 57.5 C, 45 sec; 72 C, 45 sec) with forward 5′-TCTCTGTGGCGTGTTCTCTG-3′ and reverse 5′-CACTGCAGCCCCTCACTATT-3′ primers; SCCA, (26 cycles; 94 C, 30 sec; 57.5 C, 45 sec; 72 C, 45 sec) with forward 5′-TGATTTTGCAAATGCTCCAG-3′ reverse and 4 5′-TGGTTCTCAACGTGTCCTTG-3′ primers; Interferon 56 kDa, (26 cycles; 94 C, 30 sec; 57.5 C, 45 sec; 72 C, 45 sec) with forward 5′-GCTTCAGGATGAAGGACAGG-3′ and reverse 5′-GAAATTCCTGAAACCGACCA-3′ primers; GAPDH (23 cycles; 94 C, 30 sec; 55 C, 30 sec; 72 C, 1 min) with forward 5′-GGTGAAGGTCGGTGTCAACG-3′ and reverse 5′-CAAAGTTGTCATGGATGACC-3′ primers; Amphiregulin, (32 cycles; 94 C, 30 sec; 55 C, 30 sec; 72 C, 1 min) with forward 5′-TTCGCACACCTGGGTGCCAG-3′ and reverse 5′-AAGAGGATCCACTCATCATTTATGGCTATG-3′ primers; Integrin α7B, (30 cycles; 94 C, 30 sec; 53 C, 45 sec; 72 C, 45 sec) with forward 5′-GGTGAAGCTTCCTCGGGAAGAC-3′ and reverse 5′-GGAGCAAGCTTGAGTCAGTGACAC-3′ primers; CRABP-II, (30 cycles; 94 C, 30 sec; 53 C, 45 sec; 72 C, 45 sec) with forward 5′-GACAGGATCCAGTGCTCCAGCCTAGGAG' and reverse 5′-AGAGGGATCCTGCTCTGGGCTGGTTTGG-3′ primers; 24-OH (30 cycles; 94 C, 30 sec; 55 C, 30 sec; 72 C, 1 min) with forward 5′-AAGGATCCTGTTCTGTCTTGCATCTTC-3′ and reverse 5′-CCCTAAAGCTTTCACAGCAGAGAGAAAGC-3′ primers; N-cadherin, (23 cycles; 94 C, 30 sec; 50 C, 30 sec; 72 C, 1 min) with forward 5′-TTAGTCACCGTGGTCAAACCAATC-3′ and reverse 5′-AGTGGATCCACTGCCTTCATAGTCAAACAC-3′ primers. All of the above reactions were performed in 50 μl of 2.5 mM $MgCl_2$, 50 mM KCl, and 10 mM Tris-Cl (pH 9.0) using 2.5U of *Taq* DNA polymerase (Amersham Pharmacia Biotech, Baie d'Urfé, Québec, Canada). Aliquots of 45 μl of each amplified sample were subjected to electrophoresis on 2% agarose gels containing ethidium bromide and photographed. Fluorescent bands were quantified using Kodak (Rochester, NY) digital science 1D Image Analysis software.

For Northern blotting, 20 μg of total RNA or 1 μg of poly A+ RNA were electrophoresed as described (21). Separated RNAs were transferred to a Nylon membrane (Hybond-N+, Amersham Pharmacia Biotech). The blotted membrane was

soaked in 3% SSC and 0.1% SDS at 50 C, and prehybridized at 42 C in 50 mM phosphate buffer pH 6.5, 50% formamide, 5% SSC, 10% Denhardt's solution containing 250 μg/ml sheared, and denatured salmon sperm DNA. Hybridization was carried out in the same solution by the addition of ^{32}P-labeled cDNA probes. After hybridization, the membrane was washed 4 times in 2% SSC and 0.2% SDS for 5 min, 3 times in 0.1% SSC and 0.2% SDS for 30 min at 50 C, dried, and autoradiographed. Band intensities were quantitated using the FluorChem digital imaging system and AlphaEaseFC software (Alpha Innotech Corp., San Leandro, CA).

Acknowledgments

We are grateful to Dr. Lise Binderup (Leo Laboratories, Ballerup, Denmark) for EB1089. We thank Dr. Jaroslav Novak (Montréal Genome Centre) for assistance with statistical analysis, and Dr. Leon Glass (Centre for Nonlinear Dynamics) for helpful comments on the manuscript.

Received December 20, 2001. Accepted March 26, 2002.

Address all correspondence and requests for reprints to: Dr. John H. White, Department of Physiology, McGill University, 3655 Drummond Street, Montréal, Québec H3G 1Y6, Canada. E-mail: john.white@mcgill.ca.

This work was supported by a grant from the Canadian Institutes of Health Research (CIHR; MT-15160) (to J.H.W.). R.L. was supported by a postgraduate scholarship from the CIHR. Y.N. was supported by a postdoctoral fellowship from the Heart and Stroke Foundation of Canada. R.S. is a postdoctoral fellow of the CIHR, and T.J.H. is a clinician-scientist of the CIHR. J.H.W. is a chercheur-boursier of the Fonds de Recherche en Santé du Québec (FRSQ).

REFERENCES

1. Holick MF 2001 Sunlight "D"ilemma: risk of skin cancer or bone disease and muscle weakness. The Lancet 357: 4–6
2. Slominski A, Wortsman J 2000 Neuroendocrinology of the skin. Endocr Rev 21:457–487
3. Jones G, Strugnell SA, DeLuca H 1998 Current understanding of the molecular actions of vitamin D. Physiol Rev 78:1193–1231
4. Dace A, Martin-el Yadizi C, Bonne J, Planells R, Torresani J 1997 Calcitriol is a positive effector of adipose differentiation in the OB 17 cell line: relationship with the adipogenic action of triiodothyronine. Biophys Res Commun 232:771–776
5. Hosomi J, Hosoi J, Abe E, Suda T, Kuroki T 1983 Regulation of terminal differentiation of cultured mouse epidermal cells by 1 α, 25-dihydroxyvitamin D3. Endocrinology 113:1950–1957
6. Botling J, Oberg F, Torma H, Tuohimaa P, Blauer M, Nilsson K 1996 Vitamin D3- and retinoic acid-induced monocytic differentiation: interactions between the endogenous vitamin D3 receptor, retinoic acid receptors, and retinoid X receptors in U-937 cells. Cell Growth Differ 7:1239–1249
7. Iwata K, Kouttab N, Ogata H, Morgan JW, Maizel AL, Lasky SR 1996 Differential regulation of vitamin D receptors in clonal populations of a chronic myelogenous leukemia cell line. Exp Cell Res 225:143–150
8. Nakajima H, Kizaki M, Ueno H, Muto A, Takayama N, Matsushita H, Sonoda A, Ikeda Y 1996 All-trans and 9-cis retinoic acid enhance 1,25-dihydroxyvitamin D-3-induced monocytic differentiation of U937 cells. Leukemia Res 20:665–676
9. Liu M, Lee M-H, Cohen M, Bommakanti M, Freedman LP 1996 Transcriptional activation of the Cdk inhibitor p21 by vitamin D3 leads to the induced differentiation of the myelomonocytic cell line U937. Genes Dev 10:142–153
10. Munker R, Kobayashi T, Elstner E, Norman AW, Uskokovic M, Zhang W, Andreeff M, Koeffler HP 1996 A new series of vitamin D analogs is highly active for clonal inhibition, differentiation and induction of WAF1 in myeloid leukemia. Blood 88:2201–2209
11. Zhuang, S-H, Bernstein KL 1998 Antiproliferative effect of 1α,25-dihydroxyvitamin D3 in human prostate cancer cell line LNCaP involves reduction of cyclin-dependent kinase 2 activity and persistent G1 accumulation. Endocrinology 139:1197–1207
12. Hershberger PA, Modzelewski RA, Shurin ZR, Rueger RM, Trump DL, Johnson CS 1999 1,25-Dihydroxycholecalciferol (1, 25-D3) inhibits the growth of squamous cell carcinoma and down-modulates p21(Waf1/Cip1) *in vitro* and *in vivo*. Cancer Res 59:2644–2649
13. Prudencio J, Akutsu N, Wong T, Bastien Y, Lin R, Black MJ, Alaoui-Jamali M, White JH 2001 Action of low calcemic 1,25-dihydroxyvitamin D3 analog EB1089 in head and neck squamous cell carcinoma. J Natl Cancer Inst 93:745–753
14. Muto A, Kizaki M, Yamato K, Kawai Y, Kamata-Matsushita M, Ueno H, Ohguchi M, Nishihara T, Koeffler HP, Ikeda Y 1999 1,25-dihydroxyvitamin D-3 induces differentiation of a retinoic acid-resistant acute promyelocytic leukemia cell line (UF-1) associated with expression of p21(WAF1/CIP1) and p27(KIP1). Blood 93:2225–2233
15. Bouillon R, Okamura WH, Norman AW 1995 Structure-function relationships in the vitamin D endocrine system. Endocr Rev 16:200–257
16. Guyton KZ, Kenzler TW, Posner GH 2001 Cancer chemoprevention using natural vitamin D and synthetic analogs. Annu Rev Pharmacol Toxicol 41:421–442
17. Hansen CM, Mäenpää PH 1997 EB 1089, a novel vitamin D analog with strong antiproliferative and differentiation-inducing effects on target cells. Biochem Pharmacol 54: 1173–1179
18. Mork Hansen C, Hamberg KJ, Binderup E, Binderup L, Seocalcitol (EB 1089) 2000 A vitamin D analog of anticancer potential. Background, design, synthesis, preclinical and clinical evaluation. Curr Pharmaceut Design 6:803–828
19. Koshizuka K, Kubota T, Said J, Koike M, Binderup L, Uskokovic M, Koeffler HP 1999 Combination therapy of a vitamin D3 analog and all-trans-retinoic acid: effect on human breast cancer in nude mice. Anticancer Res 19: 519–524
20. Lokeshwar BL, Schwartz GG, Selzer MG, Burnstein KL, Zhuang SH, Block NL Binderup L 1999 Inhibition of prostate cancer metastasis *in vivo*: a comparison of 1,23-dihydroxyvitamin D (calcitriol) and EB1089. Cancer Epid, Biomarkers Prev 8:241–248
21. Akutsu N, Lin R, Bastien Y, Bestawros A, Enepekides DJ, Black MJ, White JH 2001 Regulation of gene expression by 1α,25-dihydroxyvitamin D_3 and its analog EB1089 under growth inhibitory conditions in squamous carcinoma cells. Mol Endocrinol 15:1127–1139
22. Lipkin M, Newmark H, Boone CW, Kelloff GJ 1991 Calcium, vitamin D, colon cancer. Cancer Res 51: 3069–3070
23. Rubin D, Levij IS 1973 Suppression by vitamins D_2 and D_3 of hamster cheek pouch carcinoma induced with 9,10-dimethyl-1,2-benzanthracene with a discussion of the role of intracellular calcium in the development of tumors. Pathol Microbiol (Basel) 39:446–460
24. Kawaura A, Tanida N, Nishikawa M, Yamamoto I, Sawada K, Tsujiai T, Kang KB, Izumi K 1998 Inhibitory effect of 1α-hydroxyvitamin D_3 on *N*-methyl-*N'*-nitro-*N*-nitrosoguanidine-induced gastrointestinal carcinogenesis in Wistar rats. Cancer Lett 122:227–230

25. Wood AW, Chang RL, Huang M-T, Uskokovic M, Conney AH 1983 1α,25-Dihydroxyvitamin D3 inhibits phorbol ester-dependent chemical carcinogenesis in mouse skin. Biochem Biophys Res Commun 116:605–611
26. Chida K, Hashiba H, Fukushima M, Suda T, Kuroki T 1985 Inhibition of tumor promotion in mouse skin by 1α,25-dihydroxyvitamin D_3. Cancer Res 45:5426–5430
27. Hollander MC, Sheikh MS, Bulavin DV, Lundgren K, Augeri-Henmueller L, Shehee R Molinaro TA, Kim KE, Tolosa E, Ashwell JD, Rosenberg MP, Zhan Q, Fernandez-Salguero PM, Morgan WF, Deng CX, Fornace Jr AJ 1999 Genomic instability in Gadd45α-deficient mice. Nat Genet 23:176–84
28. Akutsu N, Bastien Y, Lin R, Mader S, White JH 2001 Amphiregulin is a vitamin D target gene in squamous cell and breast carcinoma. Biochem Biophys Res Commun 281:1051–1056
29. Sokal RR and Rohlf FJ 1995 Nonparametric methods in lieu of single classification ANOVAs. In: Biometry. 3rd ed. New York: Freeman; 423–439
30. Tamayo P, Slonim D, Mesirov J, Zhu Q, Kitareewan S, Dmitrovsky E, Lander ES, Golub TR 1999 Interpreting patterns of gene expression with self-organizing maps: Methods and application to hematopoietic differentiation. Proc Natl Acad Sci 96:2907–2912
31. Zou A, Elgort MG, Allegretto EA 1997 Retinoid X receptor (RXR) ligands activate the human 25-hydroxyvitamin D3-24-hydroxylase promoter via RXR heterodimer binding to two vitamin D-responsive elements and elicit additive effects with 1,25-dihydroxyvitamin D3. J Biol Chem 272: 19027–19034
32. Crawford HC, Matrisian LM, Liaw L 1998 Distinct roles of osteopontin in host defense activity and tumor survival during squamous cell carcinoma progression *in vivo*. Cancer Res 58:5206–5215
33. Quelo I, Kahlen JP, Rascle A, Jurdic P, Carlberg C 1994 Identification and characterization of a vitamin D3 response element of chicken carbonic anhydrase-II. DNA Cell Biol 13:1181–1187
34. Van Leewen, JPTM Pols HAP 1997 Vitamin D: anticancer and differentiation. In: Feldman D, Glorieux FH, Pike JW, eds. Vitamin D. Academic Press; 1093–1105
35. Kremer R, Sebag M, Champigny C, Meerovitch K, Hendy GN, White J, Goltzman D 1996 Identification and characterization of 1,25-dihydroxyvitamin D-3-responsive repressor sequences in the rat parathyroid hormone-related peptide gene. J Biol Chem 271:16310–16316
36. Chen KS, Deluca HF 1994 Isolation and characterization of a novel cDNA from HL-60 cells treated with 1,25-dihydroxyvitamin D3. Biochim Biophys Acta 1219:26–32
37. Koli K and Keskioja J 1995 1,25-dihydroxyvitmain D3 enhances the expression of transforming growth factor β-1 and its latent form binding protein in cultured breast cancer cells. Cancer Res 55:1540–1546
38. Danilenko M, Wang XN, Studzinski GP 2001 Carnosic acid and promotion of monocytic differentiation of HL60-G cells initiated by other agents. J Natl Cancer Inst 93:1224–1233
39. Diamandis EP, Yousef GM, Luo LY, Magklara A, Obiezu CV 2000 The new human kallikrein gene family: implications in carcinogenesis. Trends Endocrinol Metab 11: 54–60
40. Sotiropoulou G, Anisowicz A, Sager R 1997 Identification, cloning, and characterization of cystatin M, a novel cysteine proteinase inhibitor, down-regulated in breast cancer. J Biol Chem 272:903–910
41. Rogers MS, Kobayashi T, Pittelkow MR, Strehler EE 2001 Human calmodulin-like protein is an epithelial-specific protein regulated during keratinocyte differentiation. Exp Cell Res 267:216–224
42. Xiang RH, Hensel CH, Garcia DK, Carlson HC, Kok K, Daly MC, Kerbacher K, van den Berg A, Veldhuis P, Buys CH, Naylor SL 1996 Isolation of the human semaphorin III/F gene (SEMA3F) at chromosome 3p21, a region deleted in lung cancer. Genomics 32:39–48
43. Sekido Y, Ahmadian M, Wistuba II, Latif F, Bader S, Wei MH, Duh FM, Gazdar, AF, Lerman MI, Minna JD 1998 Cloning of a breast cancer homozygous deletion junction narrows the region of search for a 3p21.3 tumor suppressor gene. Oncogene 16:3151–3157
44. Lerman MI, Minna JD 2000 The 630-kb lung cancer homozygous deletion region on human chromosome 3p21.3: identification and evaluation of the resident candidate tumor suppressor genes. Cancer Res 60: 6116–6133
45. Vellucci VF, Germino FJ, Reiss M 1995 Cloning of putative growth regulatory genes from primary human keratinocytes by subtractive hybridization. Gene 166: 213–220
46. Suminami Y, Nagashima S, Murakami A, Nawata S, Gondo T, Hirakawa H, Numa F, Silverman GA, Kato H 2001 Suppression of a squamous cell carcinoma (SCC)-related serpin, SCC antigen, inhibits tumor growth with increased intratumor infiltration of natural killer cells. Cancer Res 61:1776–1780
47. Ramos DM, Chen B, Regezi J, Zardi L, Pytela R 1998 Tenascin-C matrix assembly in oral squamous cell carcinoma. Int J Cancer 75:680–687
48. Islam S, Carey TE, Wolf GT, Wheelock MJ, Johnson KR 1996 Expression of N-cadherin by human squamous carcinoma cells induces a scattered fibroblastic phenotype with disrupted cell-cell adhesion. J Cell Biol 135: 1643–1654
49. Zeeuwen PLJM, van Vlijmen-Willems IMJJ, Jansen BJH, Sotiropoulou G, Curfs JH, Meis JFGM, Janssen JJM, van Ruissen F, Schalkwijk J 2001 Cystatin M/E expression is restricted to differentiated epidermal keratinocytes and sweat glands: a new skin-specific proteinase inhibitor that is a target for cross-linking by transglutaminase. J Invest Dermatol 116:693–701
50. Hazan RB, Philips GR, Qiao RF, Norton L, Aaronson S 2000 Exogenous expression of N-cadherin in breast cancer cells induces cell migration, in vasion and metastasis. J Cell Biol 148:779–790
51. Tomita K, van Bokhoven A, van Leenders GJLH, Ruijter ETG, Jansen CFJ, Bussmakers MJG, Schalken JA 2000 Cadherin switching in human prostate cancer progression. Cancer Res 60:3650–3654
52. Higashino F, Yoshida K, Noumi T, Seiki M, Fujinaga K 1995 Ets-related protein E1A-F can activate 3 different matrix metalloproteinase gene promoters. Oncogene 10: 1461–1463
53. Singer AJ, Clark RAF 1999 Mechanisms of disease—cutaneous wound healing. N Engl J Med 341:738–746
54. Pilcher BK, Wang M, Qin XJ, Parks WC, Senior RM, Welgus HG 1999 Role of matrix metalloproteinases and their inhibition in cutaneous wound healing and allergic contact hypersensitivity. Ann NY Acad Sci 878:12–24
55. Agnihotri R, Crawford HC, Haro H, Matrisian LM, Havrda MC, Liaw L2001 Osteopontin, a novel substrate for matrix metalloproteinase-3 (stromelysin-1) and matrix metalloproteinase-7 (matrilysin). J Biol Chem 276: 28261–28267
56. Tian XQ, Chen TC, Holick MF 1995 1,25-Dihydroxyvitamin D3—a novel agent for wound healing. J Cell Biochem 59:53–56
57. Snellman A, Keranen MR, Hagg PO, Lamberg A, Hiltunen JK, Kivirikko KI, Pihlajaniemi T 2000 Type XIII collagen forms homotrimers with three triple helical collagenous domains and its association into disulfide-bonded trimers is enhanced by prolyl 4-hydroxylase. J Biol Chem 275:8936–8944
58. Peltonen S, Hentula M, Hagg P, Yla-Outinen H, Tuukkanen J, Lakkakorpi J, Rehn M, Pihlajaniemi T, Peltonen A 1999 A novel component of epidermal cell-matrix and

cell-cell contacts: transmembrane protein type XIII collagen. J Invest Dermatol 113:635–642
59. Cheng A, Bal GS, Kennedy BP, Tremblay ML 2001 Attenuation of adhesion-dependent signaling and cell spreading in transformed fibroblasts lacking protein tyrosine phosphate-1B. J Biol Chem 276:25848–25855
60. Borradori L, Sonnenberg A 1999 Structure sand function of hemidesmosomes: more than simple adhesion complexes. J Invest Dermatol 112:411–418
61. Green KJ, Gaudry CA 2001 Are desmosomes more than tethers for intermediate filaments? Nat Rev Mol Cell Biol 1:208–215
62. Heximer SP, Watson N, Linder ME, Blumer KJ, Hepler JR 1997 RGS2/G0S8 is a selective inhibitor of Gq α function. Proc Natl Acad Sci USA 94:14389–14393
63. Miles RR, Sluka JP, Santerre RF, Hale LV, Bloem L, Boguslawski G, Thirunavukkarasu K, Hock JM, Onyia JE 2000 Dynamic regulation of RGS2 in bone: potential new insights into parathyroid hormone signaling mechanisms. Endocrinology 141:28–36
64. Turner PR, Mefford S, Christakos S, Nissenson RA 2000 Apoptosis mediated by activation of the G protein-coupled receptor for parathyroid hormone (PTH)/PTH-related protein (PTHrP). Mol Endocrinol 14:241–254
65. Amizuka N, Kwan MY, Goltzman D, Ozawa H, White JH 1999 Vitamin D3 differentially regulates parathyroid hormone/parathyroid hormone-related peptide receptor expression in bone and cartilage. J Clin Invest 103:373–381
66. Dicker F, Quitterer U, Winstel R, Honold K, Lohse MJ 1999 Phosphorylation-independent inhibition of parathyroid hormone receptor signaling by G protein-coupled receptor kinases. Proc Natl Acad Sci USA 96:5476–5481
67. Wynick D, Small CJ, Bloom SR, Pachnis V 1998 Targeted disruption of the murine galanin gene. Ann NY Acad Sci 863:22–47
68. Lecka-Czernik B, Moerman EJ, Jones RA, Goldstein S 1996 Identification of gene sequences overexpressed in senescent and Werner syndrome human fibroblasts. Exp Gerantol 31:159–174
69. Liu, ZY, Ganju RK, Wang GF, Ona MA, Hatch WC, Zheng T, Avraham S, Gill P, Groopman JE 1997 Cytokine signaling through the novel tyrosine kinase RAFTK in Kaposi's sarcoma cells. J Clin Invest 99:1798–1804
70. Wang JF, Ganju RK, Liu ZY, Avraham H, Avraham S, Groopman JE Signal transduction in human hematopoietic cells by vascular endothelial growth factor related protein, a novel ligand for the FLT4 receptor. Blood 90: 3507–3515
71. Sampath D, Winneker RC, Zhang ZM 2001 Cyr61, a member of the CCN family, is required for MCF-7 cell proliferation: Regulation by 17β-estradiol and overexpression in human breast cancer. Endocrinology 142: 2540–2548
72. Ikematsu S, Yano A, Aridome K, Kikuchi M, Kumai H, Nagano H, Okamoto K, Oda M, Sakuma S, Aikou T, Muramatsu H, Kadomatsu K, Muramatsu T 2000 Serum midkine levels are increased in patients with various types of carcinomas. Br J Cancer 83:701–706
73. Becker MN, Diamond G, Verghese MW, Randell SH 2000 CD14-dependent lipopolysaccharide-induced ss-defensin-2 expression in human tracheobronchial epithelium. J Biol Chem 275:29731–29736
74. Townsend MJ, Fallon PG, Matthews DJ, Jolin HE, McKenzie ANJ 191 2000 T1/ST2-deficient mice demonstrate the importance of T1/ST2 in developing primary T helper cell type 2 responses. J Exp Med 1069–1075
75. Luboshits G, Shina S, Kaplan O, Engelberg S, Nass D, Lifshitz-Mercer B, Chaitchik S, Keydar I, Ben-Baruch A 1999 Elevated expression of the CC chemokine regulated on activation, normal T cell expressed and secreted (RANTES) in advanced breast carcinoma. Cancer Res 59:4681–4687
76. Giustizieri ML, Mascia F, Frezzolini A, De Pita O, Chinni LM, Giannetti A, Girolomoni G, Pastore S 2001 Keratinocytes from patients with atopic dermatitis and psoriasis show a distinct chemokine production profile in response to T cell-derived cytokines. J Allergy Clin Immunol 107:871–877
77. Petersen AB, Gniadecki R, Vicanova J, Thorn T, Wulf HC 2000 Hydrogen peroxide is responsible for UVA-induced DNA damage measured by alkaline comet assay in HaCaT keratinocytes. J Photochem Photobiol 59:123–131
78. Peus, D, Meves, A, Pott, M, Beyerle, A, Pittelkow MR 2001 Vitamin E analog modulates UVB-induced signaling pathway activation and enhances cell survival. Free Rad Biol Med 30:425–432
79. Hondal RJ, Ma S, Caprioli RM, Hill KE, Burk RF 2001 Heparin-binding histidine and lysine residues rat selenoprotein P. J Biol Chem 276:15823–15831
80. Hu SI, Carozza M, Klein M, Nantermet P, Luk D, Crowl RM 1998 Human HtrA, an evolutionarily conserved serine protease identified as a differentially expressed gene product in osteoarthritic cartilage. J Biol Chem 273: 34406–4412
81. Ramos-Gomez M, Kwak MK, Dolan PM, Itoh K, Yamamoto M, Talalay P, Kensler TW 2001 Sensitivity to carcinogenesis is increased and chemoprotective efficacy of enzyme inducers is lost in nrf2 transcription factor-deficient mice. Proc Natl Acad Sci USA 98: 3410–3415
82. Long II DJ, Waikel RL, Wang X-J, Roop DR Jaiswal AK 2001 NAD(P)H: quinone Oxidoreductase 1 deficiency and increased susceptibility to 7,12-Dimethylbenz[a]-anthracene-induced carcinogenesis in mouse skin. J Natl Cancer Inst 93:1166–1170
83. Powis G, Montfort WR 2001 Properties and biological activities of thioredoxins. Annu Rev Biophys Mol Struct 30:421–455
84. Rahman Q, Abidi P, Afaq F, Schiffmnn D, Mossman BT, Kamp DW, Athar M 1999 Glutathione redox system in oxidative lung injury. Crit Rev Toxicol 29:543–568
85. Koren R, Hadari-Naor I, Zuck E, Rotem C, Liberman UA, Ravid A 2001 Vitamin D is a prooxidant in breast cancer cells. Cancer Res 61:1439–1444
86. Carlberg C, Quack M, Herdick M, Bury Y, Polly P, Toell, A 2001 Central role of VDR conformations for understanding selective actions of vitamin D analogs. Steroids 66:213–221
87. Novak JP, Sladek R, Hudson TJ 2001 Characterization of variability in large-scale gene expression data: implications for study design. Genomics 79:104–113
88. Petrecca K, Miller DM, Shrier A 2000 Localization and enhanced current density of the Kv4.2 potassium channel by interaction with the actin-binding protein filamin. J Neurosci 20:8736–8744
89. Petraki CD, Karavana VN, Skoufogiannis PT, Little SP, Howarth DJC, Yousef GM, Diamandis EP 2001 The spectrum of human kallikrein 6 (zyme/protease M/neurosin) expression in human tissues as assessed by immunohistochemistry. J Histochem Cytochem 49:1431–1441